Gyrator Realization Based on a Capacitive Switched Cell

Doron Shmilovitz, *Member, IEEE*

***Abstract*—Efficient power gyrator realization by means of a controlled switch cell is presented. It is shown that a switching cell may be controlled so as to acquire low-frequency gyrative characteristics (on average). A realization suitable for operation with current sources is presented, that employs a switched capacitor. Due to the capacitive input, a gyrator of this nature is suitable for operation with current sources. The main applications of such gyrators are expected in superconductive magnetic energy storage systems and current-fed converters, due to the stiff-current characteristic imposed by a magnetic storage element. Other possible applications include sources with softer i–v characteristics, such as photovoltaic generators and sources of significant output inductance.**

***Index Terms*—Current converters, degenerated gyrator, duality, gyrators, power sources, time variable transformer, two-port power conservative.**

I. Introduction

THE gyrator is a passive loss-less storage less two-port network defined by the admittance matrix Y_g [1]–[8]

$$[Y_g] = \begin{bmatrix} 0 & g(t) \\ -g(t) & 0 \end{bmatrix}. \tag{1}$$

A gyrator is depicted schematically in Fig. 1. The main property of the gyrator is that it converts a one-port network N into N^d, its dual with respect to the gyration conductance $\boldsymbol{g}$, [1], [2], defined by

$$\left[v^d, i^d\right] \in N^d(g) \leftrightarrow i^d = gv, \qquad i = gv^d, \qquad [v, i] \in N.$$

Most of the practical gyrator realizations are based on a combination of two-linear amplifiers, resulting in low (usually below 0.5) conversion efficiency. Such realizations are therefore suitable for signal processing applications, rather than power processing applications.

It has been found that switched-mode converters facilitate the synthesis of loss-free (in principle only) gyrators [1], [3], [4]. Other realizations suitable for power processing include series resonant converters [5], the inverse dual converter (IDC) [6] and the $\lambda/4$ switched-mode transmission line [7], [8]. The IDC is suitable for handling the stiff current source type characteristics presented by superconducting coils [6] whereas the $\lambda/4$ gyrator was incorporated for the stabilization of loads with voltage source characteristics such as high-intensity discharge (HID) lamps [8].

Manuscript received January 20, 2003; revised May 11, 2006. This work was supported in part by the Israeli Ministry of National Infrastructure and Energy under Grant 551-171. This paper was recommended by Associate Editor I. A. Hiskens.

The author is with the School of Electrical Engineering, Tel Aviv University, 69978 Tel Aviv, Israel (e-mail: shmilo@eng.tau.ac.il).

Digital Object Identifier 10.1109/TCSII.2006.885394

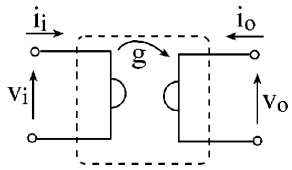

Fig. 1. Symbolic representation of a gyrator.

Efficient gyrators applied for voltage-source-into-current-source characteristics conversion are sometimes referred to as current converters [9], [10]. The need for such characteristic transformation emerged due to negative impedance loads, such as gas discharge devices (spark gapes, arcs, gas lasers), which need to be energized by a source with stabilized current, while most of the sources have a voltage source characteristic, [3], [8]. This need can be accomplished through the coupling of the voltage source to the load by means of a gyrator, which transforms the voltage source into a current source at the load side (by duality principle [9]).

For these purposes, a realization based on an inductive switching cell seems to be a good choice due to the high efficiency and flexible control, which can be obtained [3]. However, an inductive switching-cell-based gyrator is not suitable for the transformation of current sources into voltage sources due to the large voltage spikes that would be generated by the interaction between the switched inductor and the current source applied to the input terminal. Since "natural" current sources are rare, little attention has been paid to gyrators suitable for conversion of current sources into voltage sources. In superconductive magnetic energy storage systems (SMES), there is a need for current into a voltage source transformation, due to the fact that the SMES has current-source like characteristics, while most conventional loads require stabilized voltage. A gyrator based on a capacitive switching cell is suitable for that purpose, since a capacitive switching cell can accept a current source without inducing large voltages.

The concept "degenerated gyrator" is introduced in this paper, which is shown to be more suitable for modeling some switched-mode converters with regulated output (rather than the frequently employed transformer model). Realization of gyrators by means of output voltage controlled power conservative network and by means of output current controlled power conservative network are shown in Section II. The concept of "degenerated gyrator" is introduced in Section III, which is shown to well describe the average behavior of some regulated output switched circuits. Gyrator realization by an appropriate control of switched cell is given in Section IV. In Section V, it is shown how a switched capacitive cell acquires conventional gyrator characteristics on average basis by means of appropriate control.

II. Control Implied Gyrator

Power gyrators may be achieved due to inherent physical properties of the gyrator network components, such as in [4], [6], [8], which are referred to as "natural gyrators." Other gyrator realizations are achieved by means of control, such as in [3], which will be referred to as "control implied gyrators."Here we are dealing with a control implied gyrator realization.

The fact that the gyrator is a loss free storage less network suggests that its efficient realization may be based on a power conservative "black box," denoted by POPI ($P_o = P_i$) [3] whose power throughput should be controlled by means of a control parameter, S. Based on the output-controlled parameter, two types of POPI network elements are defined, the output current controlled type POPI, denoted by I-POPI (2) and the output voltage controlled POPI, denoted by V-POPI (3) as follows:

$$\left.\begin{array}{l} p_i = p_0 \quad \forall t \\ i_0 = h_I\ (s) \end{array}\right\} \tag{2}$$

$$\left.\begin{array}{l} p_i = p_0 \quad \forall t \\ v_0 = h_V\ (s) \end{array}\right\}. \tag{3}$$

$s(t)$ is a control signal which drives internal parameters of the POPI box so that (2) or (3) are obeyed. h_I and h_V are derived by inherent properties of the switching cell that define the POPI output current or voltage respectively. A gyrator based on an I-POPI type of "black box" is suitable for coupling voltage sources, which calls for a switching inductor realization. A V-POPI "black box" implies synthesis of a gyrator that is suitable for coupling current sources, which calls for realization by means of a capacitive switching cell.

Controlling a POPI network in such a way that either one of the gyrators (4) or (5) is obeyed, guarantees gyrative operation (the second equation will be automatically satisfied due to the power conservation property of the POPI)

$$i_i = g v_0 \tag{4}$$

$$i_o = -g v_i. \tag{5}$$

The control signal, which causes the I-POPI to obey the gyrator equations, is given by

$$s(t) = h_I^{-1}(-g v_i) \tag{6}$$

where $h_I^{-1}(x)$ denotes the inverse function of $h_I(x)$. In the case of V-POPI, the suitable control signal is given by (7) or (8) where $h_V^{-1}(x)$ is the inverse function of $h_V(x)$

$$s(t) = h_V^{-1}\left(\frac{i_i}{g}\right) \tag{7}$$

$$\left.\begin{array}{c} s(t) = h_V^{-1}(i_i \cdot r_g) \\ r_g \equiv \frac{1}{g} \end{array}\right\}. \tag{8}$$

Equations (5)–(7) indicate that the gyrator can be realized by the combination of a POPI "black box" and a signal processing circuit (SPC), which produces an appropriate control signal $s(t)$. It is assumed that the SPC consumes no power. In practical cases, the inverse functions $h_I^{-1}(x)$ and $h_V^{-1}(x)$ will be generated via a negative feedback loop. Loss-free gyrator realizations based on I-POPI and V-POPI are shown in Figs. 2 and 3, respectively.

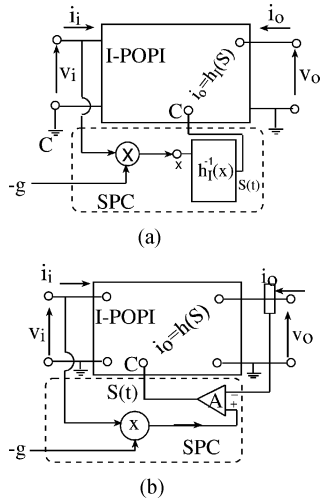

Fig. 2. I-POPI gyrator realization by means of (a) the inverse characteristic function h_I and (b) via a negative feedback control loop.

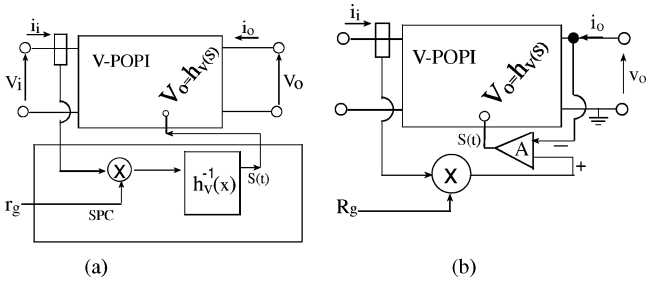

Fig. 3. V-POPI gyrator realization by means of (a) the inverse characteristic function h_v and (b) via a negative feedback control loop.

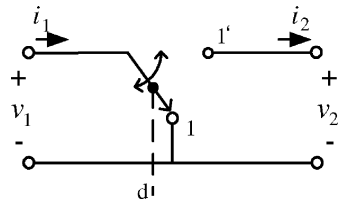

Fig. 4. Basic switching cell.

In the case of V-POPI realization, it would be rather convenient to refer to the $[Z]$ matrix of the gyrator

$$\left.\begin{array}{c} [Z_g] = \begin{bmatrix} 0 & -r_g \\ r_g & 0 \end{bmatrix} \\ r_g \equiv \frac{1}{g} \end{array}\right\}. \tag{9}$$

III. Controlled Switch and its Stabilized Output Gyrator Model

Consider a basic switching cell, which switches periodically between position 1 and 1' with a switching period T_S and a duty ratio $d(t)$, as shown in Fig. 4.

The value of $d(t)$ is set externally and is in the range of [0-1]. A moving average operator, $\langle\,\rangle_{T_S}$ is applied to instantaneous signals around the switching cell, such as a voltage $v(t)$, defined as

$$\langle v(t)\rangle_{T_S} = \frac{1}{T_S}\int_{t}^{t+T_S} v(t')dt'. \tag{10}$$

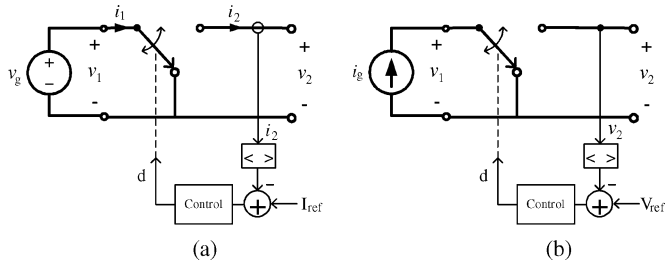

Fig. 5. Altered source characteristics via (a) stabilized output current and (b) stabilized output voltage.

Applying the averaging operator yields

$$\begin{cases} \langle v_1(t)\rangle_{T_S} = (1-d)\cdot\langle v_2(t)\rangle_{T_S} \\ \langle i_2(t)\rangle_{T_S} = (1-d)\cdot\langle i_1(t)\rangle_{T_S}. \end{cases} \tag{11}$$

These equations describe a transformer with the special properties of a dc coupling capability and an adjustable transfer ratio (equal to the external control variable, $(1-d(t))^{-1}$), [1], [5]. It may thus be concluded that a periodically exercised switch in open loop (when the duty ratio is not controlled) may be modeled as a time variable transformer. Indeed, modeling of an averaged switch as a transformer is common as it is a "natural" property of the switch [5].

Some control schemes change the switch average model. Applications that require energizing the load by a current source (such as laser diodes and LEDs), while the actual source is a voltage source, imply control of the output current as shown in Fig. 5(a). Another case is when the physical source possess current source characteristics and the load requires stabilized voltage, [11]–[13], see Fig. 5(b).

In both of these cases, the source characteristics are basically altered to its dual. The controlled switch converts a voltage source into a current source [Fig. 5(a)] or a current source into a voltage source [Fig. 5(b)] on an average basis. Applications of a controlled switched cell which converts a current source into a voltage source are not common since current sources are rare. Yet some such applications do exist, such as interfacing with SMES coils which have current source characteristics or photovoltaic generators, which in a certain operation region may be viewed as current sources,[11]–[13]. The output controlled voltage [Fig. 5(b)] implies

$$\langle v_2(t)\rangle_{T_S} = V_{\text{ref}}. \tag{12}$$

Conversion of a current source into a voltage source (or that of a voltage source into a current source) is not described well by a transformer model, since a transformer does not alter the source nature. A gyrator model is more suitable as it converts network elements into their dual ones, i.e., it converts current sources into voltage sources (and vice versa). In most practical cases, circuits which convert current sources into voltage sources (as well as those which convert voltage sources into current sources) have a regulated output. This implies a varying gyration transconductance that depends on the input independent parameter (i_1 or v_1) and on the reference signal (V_{ref} or I_{ref}, respectively), as in (13) and (14). In the case of stabilized output current

$$\left.\begin{matrix} i_2 = g\cdot v_1 \\ i_2 = I_{\text{ref}} \end{matrix}\right\} \Rightarrow g = \frac{I_{\text{ref}}}{v_1}. \tag{13}$$

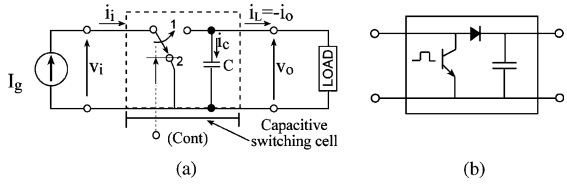

Fig. 6. (a) Capacitive switched cell. (b) Switch implementation.

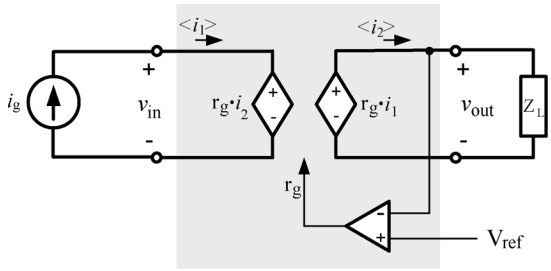

Fig. 7. Degenerated gyrator model of the regulated output switched cell.

Whereas in the case of regulated output voltage

$$\left.\begin{matrix} v_2 = r_g\cdot i_1 \\ v_2 = V_{\text{ref}} \end{matrix}\right\} \Rightarrow r_g = \frac{V_{\text{ref}}}{i_1}. \tag{14}$$

Such a type of gyrator can be regarded as a gyrator operating in a particular operation mode (or as a "degenerate" gyrator) in which the gyration transconductance is internally programmed by the preset regulated output parameter (reference signal) and the input independent parameter. In cases in which the load contains significant capacitance (as in the case of a large dc bus load [12]) the average and the instantaneous output voltages are pretty close

$$\langle v_2(t)\rangle_{T_S} \cong v_2(t). \tag{15}$$

In other cases, a capacitor must be added across the switch output port to filter the output voltage in compliance with (13), [13]. As a result, averaging of the output voltage in the control loop is not needed in this case. The capacitive switched cell formed by the addition of the filter capacitor and the switch implementation are depicted in Fig. 6. Applying either one of the control schemes depicted in Fig. 6 to the switch cell transforms the source characteristics into its dual one, which is a gyrator property. However it is a particular case of gyrator in which the output is fixed (stabilized).

This may be modeled by a gyrator with load-dependent gyration ratio as implied by (13) and (14).

In this case, the gyration ratio g (or the transresistance r_g) is no longer an independent variable. This variable is actually determined internally in correspondence to the source and reference value (which is the independent variable, see Fig. 7).

The switch configuration implies

$$i_L = d'\cdot i_i. \tag{16}$$

For instance, let us assume a pure resistive load type ($Z_L = R_L$). Equation (16) implies a gyrator model with transconductance equal to

$$r_g = R_L\cdot d'. \tag{17}$$

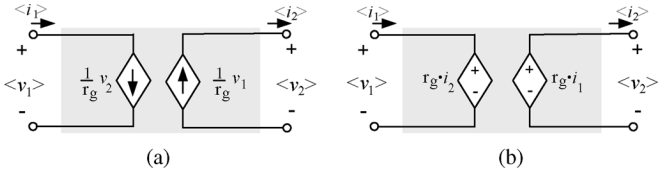

Fig. 8. Two possible gyrator models.

Substitution of (17) into (14) yields the duty cycle variation

$$d = 1 - \frac{V_{\text{ref}}}{i_g \cdot R_L}. \tag{18}$$

In most practical cases, there is a need for a regulated output parameter (either voltage or current), in which case the degenerated gyrator model, described above, applies. Yet, the switched cell may be controlled in such a manner that a real power gyrator will be created. This might be applicable for reactive VAR compensation and for changing a reactive component characteristic behavior (such as emulating a capacitor by means of an inductor).

IV. Controlled Switch Gyrator

A real power gyrator may be created by applying the control scheme of Fig. 4(b) to the average values of the switch cell (depicted in Fig. 7). In this case r_g becomes the external control variable rather than the reference value in the case of the degenerated gyrator (or d in the case of a simple, open loop operated switch, which models as a transformer). It is sufficient to implement one of the two gyrators, (4) or (5), since the second follows automatically due to power conservation. Since the switching cell does not include dissipative elements, nor sources or storage components, it is obviously a power conservative element. Substituting (4) and (5) to (11) yields (19). $\langle v_2(t)\rangle_{T_S}$ is found by equating the average input and output powers

$$\langle v_1(t)\rangle_{T_S} = r_g \langle i_2(t)\rangle_{T_S} \tag{19}$$

$$\langle v_2(t)\rangle_{T_S} = r_g \langle i_1(t)\rangle_{T_S}. \tag{20}$$

It can thus be concluded that a gyrator is realized on an average basis, which has independently adjustable gyration impedance r_g. This gyrator may be modeled by either one of the schemes in Fig. 8.

V. Simulation Results

PSPICE simulation results are provided in Figs. 9–12, which validate the proposed switched capacitor gyrator. In principle, the simulated circuit is similar to the one shown in Fig. 6. However, improved dynamical response was obtained using two single pole dual through (SPDT) switches rather than one (which implies improved capacitor charge control, since the injected current direction may be reversed with respect to the capacitor). The gyration conductance was set to $g = 0.5$. To clearly demonstrate the gyrators operation, a pure 100 mH inductor was used as a load at the gyrator output. It should be noted that the actual input voltage is pulsating therefore its moving averaged value is presented in Figs. 9 and 12. First a 10 A constant current source was applied at the gyrator input

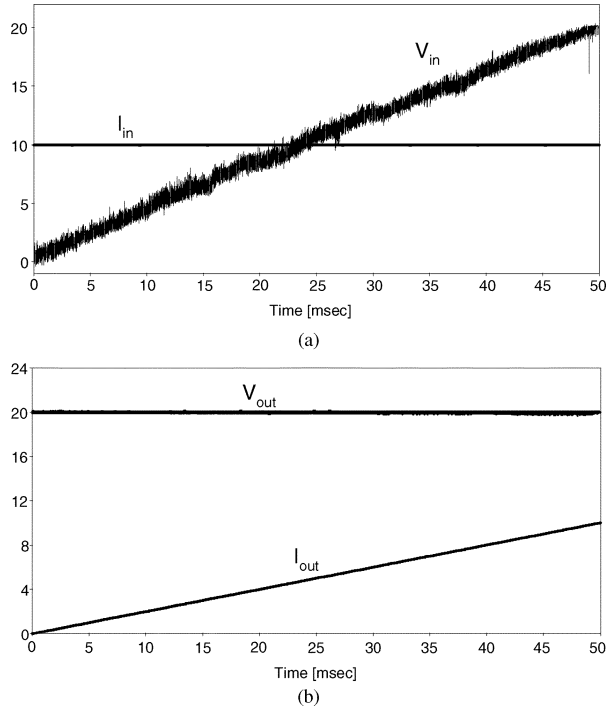

Fig. 9. Simulation results for $g = 0.5$, $L = 100$ mH, $I_{\text{in}} = 10$ A. (a) Input current and voltage (b) Output current and voltage.

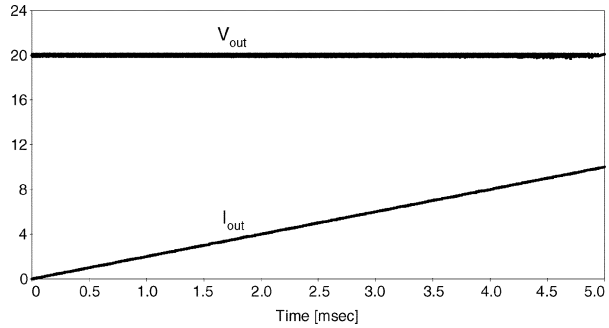

Fig. 10. Simulation results: output current and voltage for $g = 0.5$, $L = 10$ mH, $I_{\text{in}} = 10$ A.

as shown in Fig. 9. The load inductor is "seen" at the gyrator input as an equivalent capacitor C_e

$$C_e = g^2 L = 0.5^2 \cdot 100 \text{ mH} = 25 \text{ mF}. \tag{21}$$

Therefore, the input voltage ramps linearly with a slope of 400 V/s, see Fig. 9. At the output, the 10-A current source is reflected as a 20-V voltage source. As a result, the inductor current ramps with a slope of 200 A/s

$$\left(\frac{V}{L} = \frac{20 \text{ V}}{100 \text{ mH}} = \frac{200 \text{ A}}{\text{s}}\right).$$

Applying the same gyrator circuit to an inductor load of only 10 mH yields similar results, except the output current ramps with a ten times higher slope, see Fig. 10. In the second case, the constant current source was replaced by a ramp current source, which resulted in a parabolic growing input voltage, as if it was a capacitor. At the load, the ramp current source reflects as a ramp voltage source, thus the load inductor current increases parabolically, see Fig. 11. The simulation results look similar

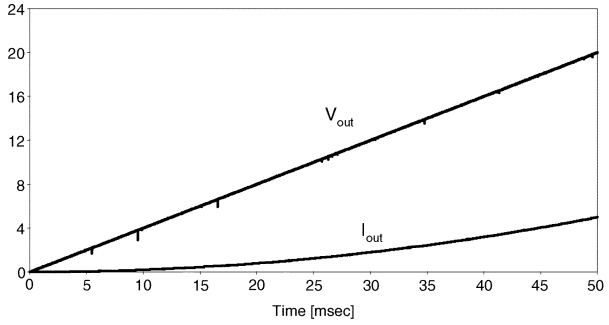

(a)

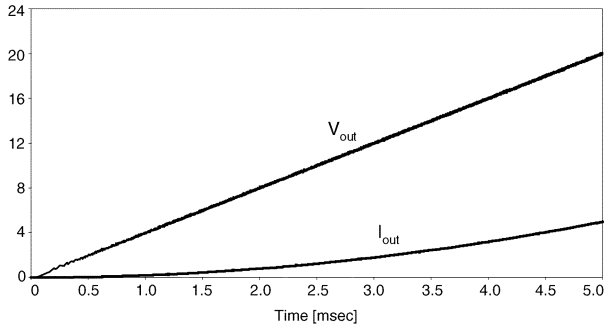

(b)

Fig. 11. Simulation results for a ramp current source ($I_{\rm in} = 200 \cdot t[A]$). (a) output current and voltage for $g = 0.5$ and $L = 100$ mH (b) output current and voltage for $g = 0.5$ and $L =$ 10mH.

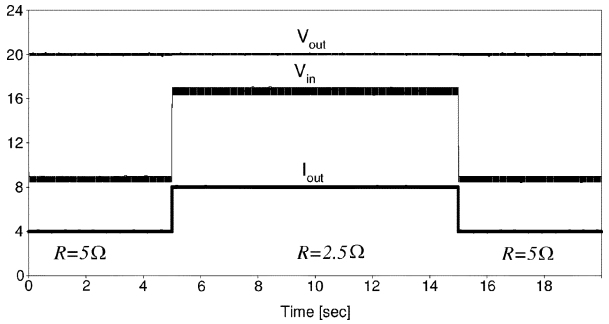

Fig. 12. Simulation results for a pulsating resistive load $I_{\rm in} = 10[A], g = 0.5$ and $R = 5\ \Omega \rightarrow 2.5\ \Omega \rightarrow 5\ \Omega$.

for both cases (for $L = 100$ mH and for $L = 10$ mH), but the simulation time is ten times longer in the first case.

The same current source was applied to a pulsating resistor load through the same switched-mode gyrator. The load was stepped from 5 to 2.5 Ω and back to 5 Ω. Simulation results are presented in Fig. 12. Since the source is constant (10 A) and $g = 0.5$, the output voltage is constant and equals 20 V. The output current is straightforward; it steps from 4 to 8 A and back to 4 A as the load steps 5 to 2.5 Ω and back to 5 Ω. The interesting load-inversion property of the gyrator may be seen through the input voltage waveform. The input is fed by a constant current source . And, the input voltage steps up when the load resistor steps down and vice versa. The resistor load R reflected to the gyrators input is

$$R_{\rm in} = \frac{1}{g^2 \cdot R}. \tag{22}$$

Thus, as the load resistor goes through the values $R = 5 \rightarrow 2.5 \rightarrow 5\ \Omega$ its' reflected value at the gyrator input acquires the values: $R_{\rm in} = 0.8 \rightarrow 1.6 \rightarrow 0.8\ \Omega$

VI. Discussion

It has been shown that switched-mode converters, under certain control schemes, exhibit gyrator characteristics. The concept of degenerated gyrator was introduced, which applies to some practical converters with regulated output [11]–[13]. The capacitive switched cell has been shown to be suitable for operation with current source supply, as well as with softer supply characteristics, such as photovoltaic arrays. However, it is not suitable for operation with stiff voltage sources. A gyrator based on such a converter is suitable for the conversion of inductors into equivalent capacitors and for the conversion of current sources into voltage sources. Such a two-port network can find applications in an SMES, as well as in reactive VAR compensation systems.

This work calls for further research regarding: conduction modes, limits of operation of the switched gyrator and range of model validity, bidirectional current conduction for operation with ac waveforms (for applications such as reactive VAR compensation).

Acknowledgment

The author acknowledges Mr. T. Israeli for his technical help.

References

[1] R. W. Newcomb, "The semistate description of non linear time-variable circuits," *IEEE Trans. Circuits Syst.*, vol. CAS-28, no. 2, pp. 62–71, Feb. 1981.

[2] A. N. Willson and H. J. Orchad, "Realization of ideal gyrators," *IEEE Trans. Circuits Syst.*, vol. CAS-21, no. 11, pp. 729–732, Nov. 1974.

[3] S. Singer, "Loss free gyrator realization," *IEEE Trans. Circuits Syst.*, vol. 35, no. 1, pp. 26–34, Jan. 1988.

[4] M. Ehsani, I. Husain, and MO. Bilgic, "Power converters as natural gyrators," *IEEE Trans. Circuits Syst. I, Fundam. Theory Appl.*, vol. 40, no. 12, pp. 946–9, Dec. 1993.

[5] R. W. Erickson and D. Maksimovic, *Fundamentals of Power Electronics*, 2nd ed. Norwell, MA: Kluwer , 2001, pp. 744–745.

[6] M. Ehsani, I. Husain, and MO. Bilgic, "Inverse dual converter (IDC) for high-power DC-DC applications," *IEEE Trans. Power Electron.*, vol. 8, no. 2, pp. 216–223, Apr. 1993.

[7] D. Shmilovitz, I. Yaron, and S. Singer, "Transmission line based gyrator," *IEEE Trans. Circuits Syst. I, Fundam. Theory Appl.*, vol. 45, no. 4, pp. 428–33, Apr. 1998.

[8] H. Ohguchi, M. H. Ohsato, T. Shimizu, and G. Kimura, "A high-frequency electronic ballast for HID lamps based on a lambda $\lambda/4$-long distributed constant line," *IEEE Trans. Power Electron.*, vol. 13, no. 6, pp. 1023–1029, Nov. 1998.

[9] R. Rabinovici and B. Z. Kaplan, "Novel DC-DC convertor schemes obtained through duality principle and topological considerations," *Electron. Lett.*, vol. 27, no. 21, pp. 1948–1950, Oct. 1991.

[10] L. Martinez-Salamero, J. Calvente, R. Giral, A. Poveda, and E. Fossas, "Analysis of a bidirectional coupled-inductor C'uk converter operating in sliding mode," *IEEE Trans. Circuits Syst. I, Fundam. Theory Appl.*, vol. 45, no. 4, pp. 355–363, Apr. 1998.

[11] A. Capel and A. Barnaba, "Evaluation of bus impedance on the spot multimission platform," *ESA J.*, vol. 7, no. 3, pp. 277–298, 1983.

[12] A. Capel, D. O'Sullivan, and J-C. Marpinard, "High-Power conditioning for space applications," *Proc. IEEE*, vol. 76, no. 4, pp. 391–408, Apr. 1988.

[13] D. Shmilovitz and S. Singer, "A switched-mode converter suitable for superconductive magnetic energy storage (SMES) systems," in *Proc. IEEE Applied Power Electron. Conf.*, Dallas, TX, Mar. 2002, pp. 630–634.